57146-54-0; $MoOBr_2(Et_2dtc)_2$, 53548-92-8; $Mo^{17}O_2(Et_2dtc)_2$, 68975-39-3; $Mo^{18}O_2(Et_2dtc)_2$, 63912-66-3; $Mo^{16}O^{17}O(Et_2dtc)_2$, 68975-40-6; $Mo^{16}O^{18}O(Et_2dtc)_2$, 68975-41-7; $Mo^{17}O^{18}O(Et_2dtc)_2$, 68975-42-8; ^{17}O, 13968-48-4.

References and Notes

(1) R. A. D. Wentworth, *Coord. Chem. Rev.*, **18**, 1 (1976).
(2) E. I. Stiefel, *Prog. Inorg. Chem.*, **22**, 1 (1976).
(3) F. A. Cotton and R. M. Wing, *Inorg. Chem.*, **4**, 867 (1965).
(4) P. W. Schneider, D. C. Bravard, J. W. McDonald, and W. E. Newton, *J. Am. Chem. Soc.*, **94**, 8640 (1972).
(5) R. R. Vold and R. L. Vold, *J. Magn. Reson.*, **19**, 365 (1975).
(6) A. D. English, J. P. Jesson, W. G. Klemperer, T. Mamouneas, L. Messerle, W. Shum, and A. Tramontano, *J. Am. Chem. Soc.*, **97**, 4785 (1975); M. Filowitz, W. G. Klemperer, L. Messerle, and W. Shum, *ibid.*, **98**, 2345 (1976).
(7) D. Samuel and B. L. Silver, *Adv. Phys. Org. Chem.*, **3**, 168 (1965).
(8) J. W. McDonald, private communication.
(9) R. R. Vold and R. L. Vold, *J. Chem. Phys.*, **61**, 4360 (1974).
(10) W. D. Kautt, H. Krüger, O. Lutz, H. Maier, and A. Nolle, *Z. Naturforsch., A*, **31**, 351 (1976).
(11) (a) B. N. Figgis, R. G. Kidd, and R. S. Nyholm, *Proc. R. Soc., London, Ser. A*, **269**, 469 (1962); (b) O. Lutz, W. Nepple, and A. Nolle, *Z. Naturforsch., A*, **31**, 978, 1046 (1976).
(12) R. J. Butcher and B. R. Penfold, *J. Cryst. Mol. Struct.*, **6**, 13 (1976).
(13) We assume the coordination environment of molybdenum to be identical with that found in each half of $(MoO_3)_2EDTA^{4-}$. See J. J. Park, M. D. Glick, and J. L. Hoard, *J. Am. Chem. Soc.*, **91**, 301 (1969).
(14) K. F. Miller and R. A. D. Wentworth, *Inorg. Chem.*, **17**, 2769 (1978).
(15) R. J. Kula, *Anal. Chem.*, **39**, 1171 (1967).
(16) H. A. Christ, P. Diehl, H. R. Schneider, and H. Dahn, *Helv. Chim. Acta*, **44**, 865 (1961).
(17) B. M. Gatehouse and P. Leverett, *J. Chem. Soc. A*, 849 (1969).
(18) L. Ricard, J. Estienne, P. Karagravanidis, P. Toledano, J. Fischer, A. Metschler, and R. Weiss, *J. Coord. Chem.*, **3**, 277 (1974). We have taken the Mo–O bond lengths of $MoO_2(Et_2dtc)_2$ to be identical with those found in $MoO_2(Pr_2dtc)_2$.
(19) B. Kamewar, M. Penavic, and C. Prout, *Cryst. Struct. Commun.*, **2**, 41 (1973).
(20) J. Dirand, L. Ricard, and R. Weiss, *J. Chem. Soc., Dalton Trans.*, 278 (1976).
(21) See, for example, W. G. Klemperer, *Angew. Chem., Int. Ed. Engl.*, **17**, 246 (1954).
(22) R. G. Kidd, *Can. J. Chem.*, **45**, 605 (1967).
(23) The total number of π bonds experienced by a metal through its d orbitals is given simply by the number of d orbitals which can participate in π bonding. The π-bond order experienced by a single ligand belonging to a set of equivalent ligands will then be the total number of π bonds experienced by the metal divided by the number of equivalent ligands. No problems occur when this principle is applied to the Mo–O bonds within an octahedron. A more complex situation, however, exists in a tetrahedral oxo complex since the e and t_2 orbitals of the metal are both capable of π bonding but to a different extent. Thus, the e orbital will contribute two π bonds of one type while the t_2 orbitals will contribute three of another type. Fortunately, the differences are easily related by a consideration of the resulting overlap populations. According to perturbation theory, these will be proportional to $[\langle\psi_{Mo}^0|\mathcal{H}|\psi_O^0\rangle G(\gamma,\pi)]/[E_{Mo}^0 - E_O^0]$, where $G(\gamma,\pi)$ is the symmetry-dependent group overlap integral and the remaining symbols have their usual meaning and refer to the d_π orbitals of molybdenum and the p_π orbitals of each oxo ligand. Since it is reasonable to assume that the matrix element is itself proportional to $G(\gamma,\pi)$, the overlap population is then proportional to $[G(\gamma,\pi)]^2$. The relative effectiveness of π bonding due to t_2 and e orbitals is then $[G(t_2,\pi)]^2/[G(e,\pi)]^2 = {}^1/_3$ if ligand–ligand overlap is neglected. The total number of equivalent π bonds experienced by the metal is then $2 + (3)(1/3) = 3$ which indicates that the π-bond order for a single Mo–O bond is 0.75. The relative effectiveness of π bonding within this tetrahedron may now be compared to that of the hypothetical octahedral complex MoO_6^{6-}. The total overlap population due to π bonding in the latter will be proportional to $3[G(t_{2g},\pi)]^2$ or $12[S(d_\pi,p_\pi)]^2$, where $S(d_\pi,p_\pi)$ is the two-atom overlap integral. The overlap population resulting from π bonding to a single ligand is then proportional to $2[S(d_\pi,p_\pi)]^2$. The total overlap population for the tetrahedral complex is proportional to $3[G(e,\pi)]^2$ or $8[S(d_\pi,p_\pi)]^2$. Since there are now only four oxo ligands, the overlap population for a single Mo–O bond is identical with that found for the octahedron. These results suggest that π-bond orders for either geometry have an equivalent basis. (See C. J. Ballhausen and H. B. Gray, "Molecular Orbital Theory", W. A. Benjamin, New York, Chapter 8.) Furthermore, application of these principles to the terminal oxo groups of $Cr_2O_7^{2-}$ (assuming with Kidd[22] that the bridging oxo ligand does not experience π bonding) and CrO_2Cl_2 results in π-bond orders of 1 and 1.5, respectively. Fortunately, the chemical shifts of these oxo ligands still vary linearly with the new π-bond orders.
(24) V. W. Day, M. F. Fredrich, W. G. Klemperer, and W. Shum, *J. Am. Chem. Soc.*, **99**, 6148 (1977).
(25) H. R. Allcock, E. C. Bissell, and E. T. Shawl, *Inorg. Chem.*, **12**, 2963 (1973).
(26) W. E. Newton and J. W. McDonald, *J. Less-Common Met.*, **54**, 51 (1977), and references therein.
(27) K. Nakamoto, "Infrared Spectra of Inorganic and Coordination Compounds", 2nd ed., Wiley-Interscience, New York, 1970, p 43.

Contribution from the Chemistry Department,
University of Virginia, Charlottesville, Virginia 22901

Infrared Spectra of the $M^+BrF_2^-$ and $M^+IF_2^-$ Ion Pairs in Solid Argon

J. HOUSTON MILLER and LESTER ANDREWS*

Received November 1, 1978

Infrared absorptions for the trihalide anions BrF_2^- and IF_2^- have been observed in experiments codepositing an argon/fluorine mixture and the alkali bromide and alkali iodide salt vapors onto a cesium iodide window at 15 K. Infrared bands in the 520–530-cm^{-1} region and the 360–365-cm^{-1} region are assigned to the symmetric $FBrF^-$ and asymmetric $BrFF^-$ species, respectively, in the $M^+BrF_2^-$ ion pair. In the alkali iodide experiments, the analogous bands were observed in the vicinity of 505 cm^{-1} for M^+FIF^- and near 355 cm^{-1} for M^+IFF^-. In most experiments, a band was observed at 550 cm^{-1} which has been previously assigned to the $M^+F_3^-$ species, a product of the secondary reaction of MF with fluorine. These results are compatible with the following reaction scheme: $MX + F_2 \rightarrow M^+XFF^- \rightarrow M^+FXF^- \rightarrow MF + XF$. Salt reactions with HF impurity also produced the M^+FHX^- bihalide complexes.

Introduction

Alkali halide salt–halogen molecule matrix reactions have been used to synthesize the trihalide species $M^+X_3^-$ including the least stable trifluoride anion.[1-3] Studies of the mixed ClF_2^-, Cl_2F^-, $ClBr_2^-$, and Cl_2Br^- species have suggested that both symmetric and asymmetric mixed $M^+X_2Y^-$ species are formed in these reactions.[1,2] Reactions of alkali bromides and iodides with fluorine were done to synthesize the new $M^+BrF_2^-$ and $M^+IF_2^-$ species which are described in this paper.

Experimental Section

The cryogenic refrigerators, vacuum systems, and high-temperature ovens have been described previously.[4] RbI, CsI, RbBr (Research Organic/Inorganic Chemical Corp.), KBr (Harshaw Chemical), KI (J. T. Baker), NaBr (Mallinckrodt), CsBr (Orion), NaCl (J. T. Baker), and NaI (Mallinckrodt) were outgassed from the Knudsen cell at or above the experimental evaporation temperature for several hours prior to the experiment. Evaporation temperatures, chosen to give 1 μ of salt vapor pressure, were CsBr (490 °C), CsI (450 °C), RbBr (460 °C), RbI (430 °C), KBr (500 °C) KI (505 °C), NaBr (520 °C), NaI (450 °C), and NaCl (520 °C). Fluorine (Matheson), after removal of condensables at 77 K, was diluted in argon to $Ar/F_2 = 400/1$ in a stainless steel vacuum system.

Fluorine samples were codeposited at 3 mmol/h with alkali halide salt vapor on an optical window at 15 K for 18–22-h periods. Infrared spectra were recorded on a Beckman IR-12 infrared spectrophotometer with an accuracy of ± 1 cm^{-1}. Samples were photolyzed with a filtered

0020-1669/79/1318-0988$01.00/0

Table I. Product Absorptions (cm^{-1}) and Intensities (Absorbance Units) Following the Matrix Reaction CsBr and F_2 and after Filtered Mercury Arc Photolysis[a]

abs	I_0	I_1	I_2	assign
313	0.18	0.26	0.30	CsF
360	0.65	0.74	0.74	Cs^+FFBr^-
389	0.04	0.09	0.1	?
407	0.1	0.1	0.09	?
415	0.1	0.1	0.1	?
435	0.27	0.23	0.22	$CsBr \cdot H_2O$
440	0.04	0.15	0.19	site
456	0.02	0.06	0.08	site
527	0.26	0.27	0.32	Cs^+FBrF^-
533	0.06	0.03	0.03	Cs^+FBrF^-
546	0.05	0.14	0.21	$Cs^+F_3^-$
550	0.24	0.02	0.02	$Cs^+F_3^-$
568	0.03	0.08	0.11	$Cs^+F_3^-$
661	0.09	0.09	0.09	BrF
721	0.03	0.03	0.03	impurity ?
744	0.17	0.17	0.17	Cs^+FHBr^-
849	0.49	0.47	0.49	Cs^+FHBr^-

[a] I_1 after 30 min of 290–1000-nm photolysis; I_2 after 30 min of 220–1000-nm photolysis.

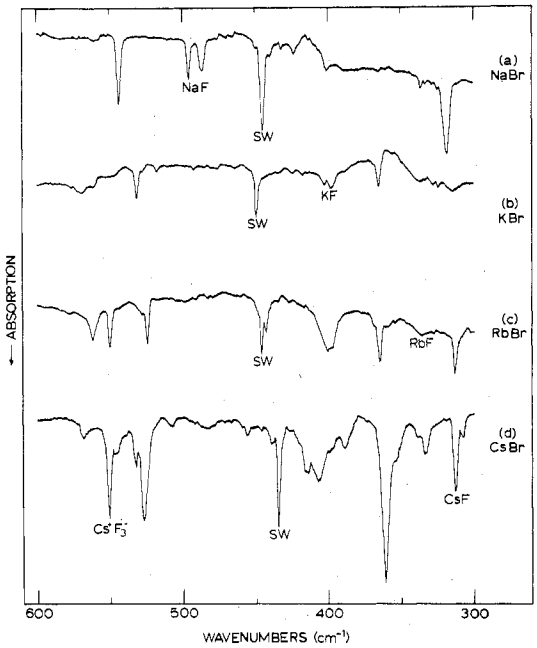

Figure 1. Infrared spectra of the products formed by codepositing alkali bromide salt vapor with $Ar/F_2 = 400/1$ samples at 15 K: (a) NaBr, (b) KBr, (c) RbBr, (d) CsBr.

BH-6 (Illumination Industries, Inc.) high-pressure mercury arc.

Results

Alkali Bromides with Fluorine. Cesium bromide salt vapor was codeposited with an $Ar/F_2 = 400/1$ sample for 21 h. The new infrared bands are listed in Table I and the spectrum is shown in Figure 1d. The major new product bands of interest appeared at 313, 360, 435, 527, and 550 cm^{-1}. In addition, a weak 660.0-, 661.5-cm^{-1} doublet due to BrF[5] and new 744- and 849-cm^{-1} bands were observed; the latter two are illustrated in Figure 2d. The 3800–4000-cm^{-1} spectral region exhibited a substantial HF impurity absorption at 3965 cm^{-1} ($A = 0.21$) in the experiment. Successive photolysis with the Pyrex (290–1000 nm) and water (220–1000 nm) filtered high-pressure mercury arc caused an increase in the 313-cm^{-1} CsF absorption,[2] slight increases in the 360- and 527-cm^{-1} bands, a marked decrease in the sharp 550-cm^{-1} $Cs^+F_3^-$ feature[2] with concomitant growth of its 546- and 568-cm^{-1} satellite bands, and a decrease in the 435-cm^{-1} $CsBr \cdot H_2O$ band[6] (labeled SW) with an increase in site splittings at 440 and 456 cm^{-1}.

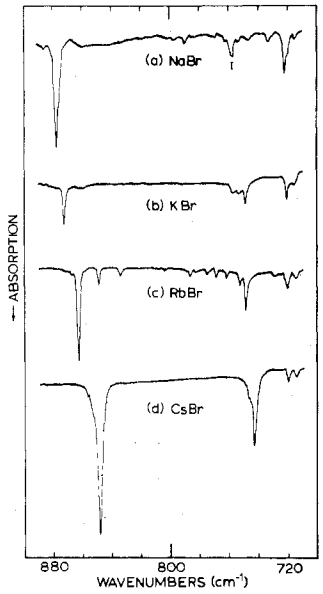

Figure 2. Infrared spectra for alkali bromide impurity HF matrix reaction products in solid argon at 15 K: (a) NaBr, (b) KBr, (c) RbBr, (d) CsBr.

Two other CsBr experiments were done using higher fluorine concentration ($Ar/F_2 = 200/1$) with a lower (450 °C) and the original (490 °C) CsBr oven temperature. The 450 °C run produced analogous but weaker absorptions whereas the latter 490 °C experiment gave stronger bands (550 cm^{-1}, $A = 0.49$, for example).

Rubidium bromide vapor was codeposited with an $Ar/F_2 = 400/1$ sample for 20 h and the infrared spectrum is illustrated in Figure 1c. The major new product bands appeared at 314, 336, 365, 447, 524, 550, and 562 cm^{-1}. Other new absorptions observed at 748 cm^{-1} ($A = 0.08$) and 863 cm^{-1} ($A = 0.23$) are shown in Figure 2c.

Potassium bromide vapor was reacted with an argon–fluorine sample for 19 h; the infrared spectrum in Figure 1b shows new bands at 364, 395, 449, and 531 cm^{-1}. Additional weak new bands were observed at 749 cm^{-1} ($A = 0.03$) and 872 cm^{-1} ($A = 0.07$), which are shown in Figure 2b. Full arc photolysis for 30 min produced new absorptions at 356 cm^{-1} ($A = 0.11$), 457 cm^{-1} ($A = 0.13$), and 527 cm^{-1} ($A = 0.04$).

Two experiments were done with sodium bromide salt vapor and the product absorptions of interest are shown at 319, 445, 486, 495, and 543 cm^{-1} in Figure 1a. Strong NaBr monomer and dimer bands were observed at 278 cm^{-1} ($A = 1.0$) and 232 cm^{-1} ($A = 0.6$)[7] and bromine monofluoride was observed at 660, 662 cm^{-1} ($A = 0.04$). Additional new absorptions at 733 cm^{-1} ($A = 0.01$), 791 cm^{-1} ($A = 0.01$), and 877 cm^{-1} ($A = 0.28$) are shown in Figure 2a. Upon thermal cycling of the sample to 30–35 K, the 319-cm^{-1} band increased ($A = 0.39 \rightarrow 0.42$), the 543-$cm^{-1}$ band grew ($A = 0.16 \rightarrow 0.22$), the 486-, 495-$cm^{-1}$ doublet due to NaF[2] decreased ($A = 0.09 \rightarrow 0.06$), the 445-$cm^{-1}$ band decreased ($A = 0.24 \rightarrow 0.20$), the 733-$cm^{-1}$ band increased ($A = 0.01 \rightarrow 0.10$), the 791-$cm^{-1}$ band increased ($A = 0.01 \rightarrow 0.03$), and the 877-$cm^{-1}$ absorption decreased ($A = 0.28 \rightarrow 0.14$). Sodium bromide vapor was deposited with argon only for 7 h and a single, sharp new band was observed at 445 cm^{-1}; this feature is reasonable for the $NaBr \cdot H_2O$ complex, labeled SW in the figure.

A final cesium bromide experiment was done for 18 h using a sample with HF added to a concentration ratio $Ar/F_2/HF = 400/1/1$. The lower frequency product bands at 313, 360, and 527 cm^{-1} were about one-fourth of the values in Table I

Table II. Product Absorptions (cm^{-1}) and Intensities (Absorbance Units) Following the Matrix Reaction between CsI and F_2 and after Filtered Mercury Arc Photolysis[a]

abs	I_0	I_1	I_2	assign
313	0.08	0.08	0.06	CsF
354	0.14	0.17	0.12	Cs^+FFI^-
399	0.09	0.09	0.09	$CsI{\cdot}H_2O$
405	0.35	0.38	0.18	$CsI{\cdot}H_2O$
420	0.12	0.19	0.07	?
447	0.14	0.08	0.26	?
504	0.09	0.09	0.06	Cs^+FIF^-
530	0.06	0.06	0.03	?
550	0.09	0.08	0.03	$Cs^+F_3^-$
562	0.07	0.07	0.13	site
568	0.04	0.06	0.04	site
605	0.04	0.03	0.0	IF
763	0.12	0.12	0.07	Cs^+FHI^-

[a] I_1 after 30 min of 290–1000-nm photolysis. I_2 after 30 min of 220–1000-nm photolysis.

for the $Ar/F_2 = 400/1$ experiment whereas the 744- and 849-cm^{-1} product absorptions were nearly the same. The higher frequency region in this experiment revealed a strong absorption at 2805 cm^{-1} ($A = 0.49$) with a shoulder at 2820 cm^{-1} and HF at 3965 cm^{-1} ($A = 0.26$).

Alkali Iodides with Fluorine. Cesium iodide vapor was reacted with argon–fluorine samples in two experiments. In the first of these, salt vapor was evaporated at 435 °C and codeposited with an $Ar/F_2 = 200/1$ sample for 20 h. The spectrum was similar to the second experiment described below except the 763-cm^{-1} ($A = 0.13$) band was slightly more intense. In the second experiment, salt was evaporated at 450 °C and codeposited with an $Ar/F_2 = 400/1$ sample for 18 h. The infrared spectrum is shown in Figure 3d and the band intensities are given in Table II. Particular attention is called to CsF at 313, 354 cm^{-1}, salt–water complex[6] at 405, 504 cm^{-1}, $Cs^+F_3^-$ at 550 cm^{-1}, and IF[8] at 604 cm^{-1}. A new band was also observed at 763 cm^{-1}. The effect of high-pressure mercury arc photolysis on the band intensities is also given in Table II.

Rubidium iodide salt vapor was reacted with an argon–fluorine mixture for 21 h. The infrared spectrum in Figure 3c shows new bands at 314, 333 (RbF), 356, 415 (SW), 504, 550, 561, and 604 cm^{-1} (IF). An additional strong, sharp band was observed at 776 cm^{-1} ($A = 0.41$). Rubidium iodide was deposited with argon from the same manifold for 19 h the next day and absorptions were observed at 415 cm^{-1} ($A = 0.50$) and 776 cm^{-1} ($A = 0.12$).

Three experiments were done with potassium iodide. A 6-h codeposition of KI with argon produced one band at 420 cm^{-1} ($A = 0.17$). Two studies of the KI and F_2 matrix reaction produced similar results which are shown in Figure 3b. The major bands appeared at 355, 370, 396 (KF), 420 (SW), 506, 558, and 604 (IF) cm^{-1}. An additional absorption was observed at 784 cm^{-1} ($A = 0.38$). The major effect of full-arc photolysis was to increase the 355-cm^{-1} band and decrease the 370-cm^{-1} absorption.

Sodium iodide vapor was deposited for 4 h with argon and a weak new band was observed at 424 cm^{-1}; this reaction was continued for 18 h more with an $Ar/F_2 = 400/1$ sample and the spectrum in Figure 3a was produced. The major new bands were observed at 327, 424 (SW), 495 (NaF), 519, and 603 cm^{-1} (IF). In addition a new absorption was observed at 795 cm^{-1} ($A = 0.05$).

Alkali Chlorides with Fluorine. The cesium chloride–fluorine matrix reaction was studied previously in this laboratory[2] and major absorptions were reported at 312, 365, 550, and 560 cm^{-1}. In addition, new bands were also observed at 826 cm^{-1} ($A = 0.04$) and 933 cm^{-1} ($A = 0.08$). Potassium chloride was codeposited with an $Ar/F_2 = 300/1$ sample for 8 h. New

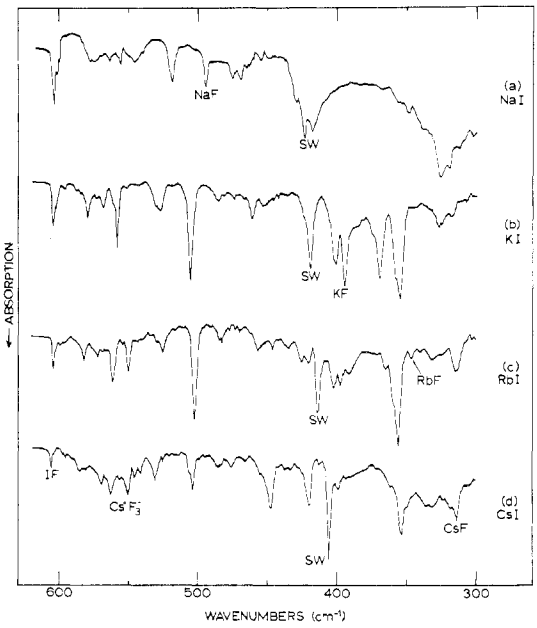

Figure 3. Infrared spectra of the products formed upon codepositing alkali iodide salt vapor with $Ar/F_2 = 400/1$ samples at 15 K: (a) NaI, (b) KI, (c) RbI, (d) CsI.

infrared product absorptions were observed at 314 cm^{-1} (0.06), 391 cm^{-1} ($A = 0.04$), 574 cm^{-1} ($A = 0.06$), and 950 cm^{-1} ($A = 0.05$), and a weak broad band appeared at 2500 cm^{-1} ($A = 0.03$) with resolved peaks at 2492 and 2547 cm^{-1}.

Sodium chloride vapor was deposited with argon and absorptions were observed at 335 cm^{-1} (NaCl)[1] and 468 cm^{-1} (SW);[1,6] reaction with an argon–fluorine sample for 18 h produced new absorptions at 308 cm^{-1} ($A = 0.43$), 495 cm^{-1} (NaF, $A = 0.13$),[2] 589 cm^{-1} ($A = 0.28$), a ClF multiplet[9] at 770, 763, and 759 cm^{-1} ($A = 0.08$), and sharp bands at 795 cm^{-1} ($A = 0.05$), 805 cm^{-1} ($A = 0.06$), and 963 cm^{-1} ($A = 0.20$). Upon photolysis, the 495-cm^{-1} band grew slightly (to $A = 0.15$) and the 963-cm^{-1} absorption decreased slightly (to $A = 0.17$). The region above 2000 cm^{-1} was not scanned in this experiment.

Discussion

The alkali halide–fluorine matrix reaction product trihalide ions will be identified and the reaction mechanism discussed.

Trihalide Ions. Earlier work from this laboratory[1-3] has provided spectroscopic characterization of the $M^+F_3^-$, $M^+Cl_3^-$, $M^+Br_3^-$, and $M^+I_3^-$ matrix-isolated ion pairs from the salt—halogen matrix reaction. A study of the CsCl and F_2 matrix reaction produced CsF and the symmetrical $Cs^+ClF_2^-$ species in addition to a possible asymmetric species Cs^+Cl–F–F^-. The present reaction product spectra were examined with counterparts of the latter two species in mind.

Bands labeled SW are clearly due to the salt–water complex on the basis of the observation of some of them in earlier work from this laboratory[1,2] and a more recent study[6] and by the systematic trends illustrated in Figures 1 and 3. In addition, the NaF, KF, RbF, and CsF absorptions are in agreement with earlier alkali fluoride work.[2] The strong, sharp $Cs^+F_3^-$ and $Rb^+F_3^-$ bands[2] at 550 cm^{-1} are also obvious in Figures 1 and 2; these products arise from the reaction of RbF and CsF, produced by the initial cocondensation reaction, with additional F_2. Photolysis confirms that several nearby sites of the trifluoride species are also observed here.

Two major new product bands were observed for each alkali bromide reaction, 360 and 527 cm^{-1} for CsBr, 365 and 524 cm^{-1} for RbBr, 364 and 531 cm^{-1} for KBr, and 319 and 543 cm^{-1} for NaBr. The higher set of bands from 527 to 543 cm^{-1} for Cs^+ to Na^+ correlates nicely with the analogous set from

Table III. Infrared Absorptions[a] (cm^{-1}) Assigned to the Symmetric M^+FXF^- and Asymmetric[b] M^+XFF^- Trihalide Species in Solid Argon at 15 K

	M^+FXF^-				M^+XFF^-		
X	Na^+	K^+	Rb^+	Cs^+	K^+	Rb^+	Cs^+
Cl	589	574	565[c]	566[c,d]	391	371[c]	365[c]
Br	543	521	524	527	364	366	360
I	520	506	503	504	357	356	354

[a] Major site absorptions. [b] The asymmetric sodium species absorbing at 308, 319, and 327 cm^{-1}, respectively, for NaCl, NaBr, and NaI reactions are believed to be $NaF\cdots FX$ complexes. [c] Reference 2. [d] It may be noticed that the $M^+ClF_2^-$ fundamentals are near the 578-cm^{-1} ClF_2 radical value (G. Mamantov, E. J. Vasini, M. C. Moulton, D. G. Vicroy, and T. Mackawa, *J. Chem. Phys.*, 54, 3419 (1971)). The present cocondensation reaction products exhibit a definite M^+ effect which indicates an ionic species. On the other hand, ClF_2 radical is formed on photodissociation of ClF_3 and ClF, F_2 with insufficient energy for photoionization.

566 to 589 cm^{-1} assigned to the symmetrical $M^+ClF_2^-$ species,[2] and accordingly, the 527–543-cm^{-1} bands are assigned to ν_3 the antisymmetric Br–F stretching mode of F–Br–F^- in the appropriate $M^+BrF_2^-$ ion pair.

Again, two major new product bands were observed for each alkali iodide reaction, 354 and 504 cm^{-1} for CsI, 356 and 504 cm^{-1} for RbI, 356 and 506 cm^{-1} for KI, and 327 and 519 cm^{-1} for NaI. The higher set of bands from 504 to 519 cm^{-1} follows the above trends for the $M^+ClF_2^-$ and $M^+BrF_2^-$ species and their assignment to ν_3, the antisymmetric I–F stretching mode, of F–I–F^- in the $M^+IF_2^-$ species is straightforward.

The trend in ν_3 modes for the presumably linear ClF_2^-, BrF_2^-, and IF_2^- anions is similar to the trend in axial antisymmetric X–F stretching modes in the XF_3 and X_2F_2 molecules.[5] The XF_2^- anion frequencies are contrasted in Table III.

Force constants calculated for the linear species F–Cl–F^-, F–Br–F^-, and F–I–F^- using the ν_3 modes at 566, 527, and 504 cm^{-1}, respectively, for the Cs^+ species give $F_r - F_{rr}$ values of 1.72, 2.11, and 2.19 mdyn/Å, respectively. It is perhaps surprising that this force constant increases with the heavier halogen; this may in part be due to a decreasing value of F_{rr} with the heavier halogen, although the interaction force constant cannot be determined since the ν_1 mode for these matrix-isolated species has not been observed.

Absorptions at 365 and 371 cm^{-1} in CsCl and RbCl studies with F_2 were also observed from CsF and RbF reactions with ClF which supported their assignment to an asymmetric Cl–F–F^- anion.[2] The lower set of bands at 360, 365, and 364 cm^{-1} in the CsBr, RbBr, and KBr reactions and at 354, 356, and 356 cm^{-1} for CsI, RbI, and KI show a very small heavy halogen shift and their assignment to the same type of X–F–F^- species is indicated. The small halogen shift suggests that the vibration is predominantly an F–F stretching mode in the asymmetric species. Observation of the bromine and iodine counterparts of the Cl–F–F^- species reported earlier[2] provides support for the identification of this unusual F-centered asymmetric trihalide anion with the heavier alkali cations.

The weaker product absorption observed in these studies with the sodium halides at 308 cm^{-1} with NaCl, 319 cm^{-1} with NaBr, and 327 cm^{-1} with NaI is probably due to a third molecular species. Examination of the spectra reveals possible heavier metal counterparts of this absorber near 300 cm^{-1}. In the chloride salt experiments, the KCl reaction yielded a band at 314 cm^{-1}, RbCl produced a new 306-cm^{-1} absorption, and CsCl gave a new 298-cm^{-1} band previously attributed[2] to another matrix site of CsF. In the bromide salt experiments, a new band was observed at 314 cm^{-1} in the RbBr study, a weak broad feature appeared at 317 cm^{-1} in the KBr experiment, and a 308-cm^{-1} shoulder was found on the CsF band at 313 cm^{-1} in the CsBr work. In the iodide salt experiments, a weak feature 325 cm^{-1} was produced with KI, and a 314-cm^{-1} absorption was observed with RbI. These product absorptions between 298 and 327 cm^{-1} show little shift with alkali cation or with the heavier halogen which suggests a vibration primarily involving fluorine. These absorptions are tentatively attributed to a fluoride–fluorine stretching mode in a $M^+F^-\cdots F-X$ complex, formed by decomposition of the asymmetric trihalide species M^+F-F-X^-.

Table IV. Major Sharp Product Absorptions (cm^{-1}) Assigned to the M^+FHX^- Species from the Matrix Reaction of HF and MX Molecules[a]

	$FHCl^-$	$FHBr^-$	FHI^-
Na^+	963	877	795
K^+	950	872	784
Rb^+	946	863	776
Cs^+	933	849	763

[a] Minor sharp bands were also observed at 733, 749, 748, and 744 cm^{-1}, respectively, for the NaBr-, KBr-, RbBr-, and CsBr-HF reaction products.

The overall matrix reaction, as proposed for the analogous alkali chloride–fluorine matrix reactions,[2] is described in reactions 1 and 2 for the bromide and iodide salts. The present

$$CsBr + F_2 \rightarrow \underset{Cs^+}{Br-F-F^-} \rightarrow \underset{Cs^+}{F-Br-F^-} \rightarrow CsF + BrF \quad (1)$$

$$CsI + F_2 \rightarrow \underset{Cs^+}{I-F-F^-} \rightarrow \underset{Cs^+}{F-I-F^-} \rightarrow CsF + IF \quad (2)$$

observations cannot rule out an insertion mechanism for the formation of the symmetrical F–X–F^- species but this appears less likely. The matrix reaction probably first forms the asymmetric trihalide ion observed in the 350–390-cm^{-1} range for chloride, bromide, and iodide salts of K^+, Rb^+, and Cs^+. The smaller Na^+ ion apparently cannot stabilize the asymmetric trifluoride species, and although Na^+ does support the rearrangement to the symmetric trihalide anion, the $Na^+F^-\cdots FX$ complex is the dominant product. The alkali fluoride and BrF or IF were also observed for all reactions confirming that collision complexes of the type proposed here are required for the formation of these final products of reactions 1 and 2. The present NaCl reaction with F_2 also produced NaF and ClF further substantiating this mechanism.

It is proposed that the symmetrical

$$\underset{M^+}{(F-Br-F)^-} \quad \text{and} \quad \underset{M^+}{(F-I-F)^-}$$

species are "T" shaped with a linear anion centered over the alkali cation. The asymmetric trihalide species

$$\underset{M^+}{Br-F-F^-} \quad \text{and} \quad \underset{M^+}{I-F-F^-}$$

species probably contain linear anions, but the M^+ ion is more likely to reside nearer the more electronegative terminal fluorine atom. This possible cation–anion structure facilitates the decomposition to the alkali fluoride–halogen fluoride complex $M^+F^-\cdots FX$ or further to the isolated products of reactions 1 and 2.

Bihalide Ions. The sharp new bands between 763 and 963 cm^{-1} for each iodide, bromide, and chloride salt reaction exhibit interesting alkali metal and halide trends which are illustrated in Table IV. The position of these absorptions between the strong sharp antisymmetric hydrogen stretching absorptions of $M^+HCl_2^-$ and $M^+HBr_2^-$ and the analogous mode of the $M^+HF_2^-$ species[7,10,11] suggested their assignment as F···H···X^- species with two weak hydrogen halide bonds, which is produced by the salt reaction with HF impurity in the fluorine sample or HF formed from the reaction of F_2 with traces of H_2O in the vacuum system. This possibility was strengthened

by adding HF to the F_2 used in a final CsBr experiment which also revealed a strong, broad 2805-cm^{-1} absorption in addition to the sharp 849- and 744-cm^{-1} absorptions.

Assignment of the absorptions in Table IV to bihalide species is confirmed by recent salt reactions with HF and DF performed by Ault.[12] The interesting question remaining is the type of bihalide species responsible for the Table IV absorptions. The original observation of F–H···Br^- species by Evans and Lo[13] revealed a very strong, broad perturbed H–F stretching mode at 2900 cm^{-1} and a sharp bending mode at 740 cm^{-1}. Clearly the present 2805 and 744 cm^{-1} argon matrix absorptions are due to the type I hydrogen-bonded complex

$$\begin{matrix} F\text{–}H\cdots Br^- \\ Cs^+ \end{matrix}$$

The sharp 849-cm^{-1} band could be another bending mode of the linear F–H···Br^- ion since the Cs^+ ion will remove the degeneracy of the bending mode for the linear molecule. The relative intensities of the 2805-, 849-, and 744-cm^{-1} absorptions are constant in the present experiments and in the HF + CsBr and HBr + CsF work of Ault.[12] On the other hand, a type II hydrogen bonded species with two weak hydrogen–halide bonds, F···H···Br^-, could also be formed and stabilized by the cation, as mentioned previously, and it could reasonably be expected to exhibit an "antisymmetric" hydrogen stretching mode in this region. Studies of the isolated mixed ions in this laboratory revealed a weak 2761-cm^{-1} band for F–H···Cl^- and a weak 2961-cm^{-1} absorption for F–H···Br^-, both type I species, without new product absorptions in the 700–1000-cm^{-1} region.[14] This suggests that a bound cation is required to stabilize a type II mixed bihalide ion.

Conclusions

The cocondensation reaction of alkali bromide and iodide salt molecules with argon/fluorine mixtures has produced new infrared absorptions which are assigned to the mixed trihalide species FXF^- and XFF^-. The new absorption in the 500-cm^{-1} region attributed to the antisymmetric X–F stretching mode of the former shows considerable heavy halogen shift whereas the product in the higher 300-cm^{-1} region attributed to the F–F mode of the latter exhibits little halogen shift. The observation of alkali fluoride and XF products provides the overall reaction mechanism $MX + F_2 \rightarrow M^+XFF^- \rightarrow M^+FXF^- \rightarrow MF + XF$. Salt reactions with HF impurity also produced the bihalide species M^+FHX^-.

Acknowledgment. The authors gratefully acknowledge financial support from the National Science Foundation under Grant CHE 76-11640 and helpful discussions with Professor B. S. Ault on M^+FHX^- species before publication of his results.

Registry No. Na^+FClF^-, 62624-99-1; K^+FClF^-, 15321-05-8; Na^+FBrF^-, 69204-01-9; K^+FBrF^-, 69204-02-0; Rb^+FBrF^-, 69204-03-1; Cs^+FBrF^-, 40419-00-9; Na^+FIF^-, 69204-05-3; K^+FIF^-, 69204-06-4; Rb^+FIF^-, 69204-07-5; Cs^+FIF^-, 69204-08-6; K^+ClFF^-, 69204-09-7; K^+BrFF^-, 69204-10-0; Rb^+BrFF^-, 69204-11-1; Cs^+BrFF^-, 69204-12-2; K^+IFF^-, 69204-13-3; Rb^+IFF^-, 69204-14-4; Cs^+IFF^-, 69204-15-5; Na^+FHCl^-, 69204-16-6; Na^+FHBr^-, 69204-17-7; Na^+FHI^-, 69204-18-8; K^+FHCl^-, 69204-19-9; K^+FHBr^-, 69204-20-2; K^+FHI^-, 69204-21-3; Rb^+FHCl^-, 69204-22-4; Rb^+FHBr^-, 69204-23-5; Rb^+FHI^-, 69204-24-6; Cs^+FHCl^-, 69204-25-7; Cs^+FHBr^-, 69204-26-8; Cs^+FHI^-, 69204-27-9; CsF, 13400-13-0; $Cs^+F_3^-$, 58915-74-5; BrF, 13863-59-7; IF, 13873-84-2.

References and Notes

(1) B. S. Ault and L. Andrews, *J. Am. Chem. Soc.*, **97**, 3824 (1975); *J. Chem. Phys.*, **64**, 4853 (1976).
(2) B. S. Ault and L. Andrews, *J. Am. Chem. Soc.*, **98**, 1591 (1976); *Inorg. Chem.*, **16**, 2024 (1977).
(3) L. Andrews, E. S. Prochaska, and A. Loewenschuss, to be submitted for publication.
(4) L. Andrews, *J. Chem. Phys.*, **48**, 972 (1968); **54**, 4935 (1971).
(5) E. S. Prochaska, L. Andrews, N. R. Smyrl, and G. Mamantov, *Inorg. Chem.*, **17**, 970 (1978).
(6) B. S. Ault, *J. Am. Chem. Soc.*, **100**, 2426 (1978).
(7) B. S. Ault and L. Andrews, *J. Chem. Phys.*, **64**, 4853 (1976).
(8) B. Rosen, Ed., "Spectroscopic Data Relative to Diatomic Molecules", Pergamon Press, Oxford, England, 1970.
(9) L. Andrews, F. K. Chi, and A. Arkell, *J. Am. Chem. Soc.*, **96**, 1997 (1974).
(10) B. S. Ault and L. Andrews, *J. Chem. Phys.*, **63**, 2466 (1975).
(11) B. S. Ault, *J. Phys. Chem.*, **82**, 844 (1978).
(12) B. S. Ault, to be submitted for publication.
(13) J. C. Evans and G. Y-S. Lo, *J. Phys. Chem.*, **70**, 543 (1966).
(14) L. Andrews, S. A. McDonald, F. T. Prochaska, and G. L. Johnson, to be submitted for publication.

Contribution from the Department of Chemistry, Regional Engineering College, and Department of Applied Sciences and Humanities, Kurukshetra University, Kurukshetra 132119, Haryana, India

Magnetic and Spectral Properties of Oxovanadium(IV) Complexes of ONO Donor Tridentate, Dibasic Schiff Bases Derived from Salicylaldehyde or Substituted Salicylaldehyde and *o*-Hydroxybenzylamine

A. SYAMAL* and K. S. KALE

Received May 18, 1978

The oxovanadium(IV) complexes of Schiff bases derived from salicylaldehyde, 5-chlorosalicylaldehyde, 5-bromosalicylaldehyde, 4-methoxysalicylaldehyde, 3,5-dichlorosalicylaldehyde, 2-hydroxy-1-naphthaldehyde, and *o*-hydroxybenzylamine are synthesized and characterized by elemental analysis, infrared and electronic spectra, and magnetic susceptibility measurements from 80 to 294 K. The Schiff bases behave as tridentate, dibasic ONO donor ligands. The complexes exhibit subnormal magnetic moments (μ_{eff} = 1.10–1.23 μ_B at room temperature). The magnetic moments of the complexes decrease significantly as the temperature is lowered indicating the presence of antiferromagnetic exchange with a singlet ground state. The exchange interaction parameter, J, of the complexes is in the range −241 to −307 cm^{-1}. The complexes exhibit three electronic spectral bands at around 13 000, 18 000, and 23 000 cm^{-1} due to the transitions $d_{xy} \rightarrow d_{xz}$, d_{yz}, $d_{xy} \rightarrow d_{x^2-y^2}$, and $d_{xy} \rightarrow d_{z^2}$, respectively. The ν(V=O) frequency of the complexes is observed in the region 900–910 cm^{-1}. On the basis of magnetic susceptibility and infrared data, a dimeric structure with benzylaminophenol oxygen atoms as the bridging atoms is suggested.

Introduction

There has been considerable interest in the structural, magnetic, and spectral properties of metal(II) and -(III) complexes with tridentate, dibasic ligands in recent years.[1-4] These ligands force the metal(II) and -(III) ions to dimerize or polymerize leading to metal complexes with unusual magnetic and structural properties. Oxovanadium(IV) complexes with tridentate, dibasic Schiff bases (I) with subnormal magnetic moments have been reported, and the

* To whom correspondence should be addressed at the Regional Engineering College.

0020-1669/79/1318-0992$01.00/0